

Cooperative Autonomy of Multiple Solar-Powered Thermalling Gliders [★]

Nahum Camacho,^{*}
Vladimir N. Dobrokhodov, Kevin D. Jones,^{**}
Isaac I. Kaminer^{***}

^{} Graduate student at the Department of Mechanical and Aerospace Engineering, Naval Postgraduate School, Monterey, CA 93943 USA
(e-mail: ncamacho@nps.edu)*

*^{**} Associate Professors at the Department of Mechanical and Aerospace Engineering, Naval Postgraduate School, Monterey, CA 93943 USA (e-mail: vndobrok@nps.edu, kdjones@nps.edu)*

*^{***} Professor at the Department of Mechanical and Aerospace Engineering, Naval Postgraduate School, Monterey, CA 93943 USA
(e-mail: kaminer@nps.edu)*

Abstract: The paper presents the multidisciplinary systematic approach to the design of a fleet of cooperative gliders capable of extended endurance operation. The flock of autonomous gliders is able to harvest energy from the environment both through photo-voltaic energy generation and through exploitation of natural convective lift in the surrounding air, and acts cooperatively to meet mission requirements and to share knowledge of the local environment. The paper begins with a brief overview of the total-energy approach required for such a feat, along with a short description of key system components. This is followed by details of the evolution of a previously-developed architecture that supported autonomous thermalling, to an architecture that considers the total-energy budget in all flight segments, and optimizes the cooperative flight to maximize the cumulative energy capture while simultaneously meeting the mission objectives.

Keywords: cooperative control; solar energy; convective thermals energy; autonomous glider.

1. INTRODUCTION

Imagine a large team of gracefully soaring autonomous gliders instrumented with sensors capable of detecting and utilizing the convective air flow, and high-efficiency solar panels which are seamlessly embedded into the wings to replenish the electrical energy of onboard batteries that power avionics. The gliders are sequentially launched from a distant area and assigned to provide, for example, an extended communication network coverage or to serve as a low-orbit observation satellites for the forest fire or border protection. The gliders reach the area of operations and remain there unattended for an extended period of time, perhaps up to a year. When a need for maintenance arises the distributed intelligent algorithm then reconfigures the team of gliders and dispatches a subset of aircraft for the scheduled service; in turn, when a substitute or serviced aircraft return the same algorithm reconfigures the team to accept the new players. The distributed soaring gliders can either operate in a distributed fashion or fly together in a suitable formation to provide a more focused high-resolution support. The latter may include cooperative distributed sensing to achieve the desired sensors resolution, tracking of weather formations, border patrol, etc. that are currently provided by much larger, heavier and more expensive systems.

Despite significant advances in a number of technologies resulting in shrinking the size, weight and power (SWAP) constraints in aerospace technologies, the ability to stay aloft for extended periods of time is still remain reserved for larger systems such as AWACS and/or mid and large scale UAVs such as Predators and Global Hawks. While extremely capable either of these systems still do not provide the desired 24/7 continuous operational endurance and flexibility. Deployment of these assets requires large teams of ground personnel and has to be planned with significant and sufficient lead-time. Needless to say that the development and operational cost of those assets might be prohibitively expensive.

What if the endurance capabilities of larger aircraft and UAVs were achieved by much smaller autonomous systems with significantly less power consumption and maintenance needs? Then these smaller and cheaper UAVs would be able to carry out many missions reserved today for larger, heavier, more expensive long endurance systems. This is the precisely the objective, that has been addressed in the recent development by Andersson et al. [2012b,a]. The project concept shifts the paradigm from large, costly single point of failure platforms to distributed, small unmanned systems that can provide the same level of service at a significantly lower cost and with greater robustness. To achieve the goal, the project develops a system of multiple cooperating autonomous gliders that harvest thermal

[★] This work was supported in part by the ARL contract number and the NPS CRUSER contract number.

(convective air) and solar energy (photovoltaic) to achieve distributed collaborative sensing and dynamic area coverage according to a specific task at a significantly lower operational cost and personnel requirements (training and manning) than the existing systems.

1.1 Technical Background and Envisioned Approach

One of the most critical limiting factors impacting effective collaborative autonomy today is the lack of endurance that is typical in most of the existing autonomous aircraft. Numerous futuristic ideas and concepts will not be implemented in real life solely due to this single reason. Until R&D community realizes that the energy onboard (of either a single or a flock of agents) and the mission objectives are equally important metrics of the mission management (planning and execution), and finds a way of solving this challenge, there will not be revolutionary advances made in the area of persistent intelligent collaborative autonomy.

Despite almost two decades of significant advances in low-power and high-performance microelectronics development including CPUs, sensors, actuators, and communication circuits Tong [1995], Singh and Shukla [2010], the only task addressed was to lower the power consumption of autonomous machines and therefore to reduce the pace of energy expenditures. On the other hand, the progress of energy renewable technologies is lagging behind. Since the loss of energy is unavoidable due to the inefficiency in energy conversion, storage, and transmission, the mission duration will always be limited. However, implementing novel approaches for the cooperative mission design and execution along with the optimal energy management can not only further reduce the rate of loss of limited energy resources but also can result in energy increase during the autonomous mission execution; this capability is not readily available today in any of the available technologies, see Siciliano and Khatib [2008], Martinez et al. [2008], and Nonami et al. [2013].

Despite the complexity of the energy-management task, the practical solutions of the extended duration flight do exist in nature. Millions of years of evolution enable a number of families of birds for very long duration flights. While the fundamentals of flight are the same, the effective energy management principles during the flight do differ. One of the most extraordinary birds capable of the long duration flight is the bar-tailed godwit, a large, streamlined shorebird, that performs a non-stop across the ocean flight, see USGS [2007], of more than eight days over a distance of 7,200 miles; the distance equivalent of making a round-trip flight between New York and Paris without ever touching down. Another example is the albatross that can fly around the world with little or no flapping of their wings, see Richardson [2011]. Remarkably, some birds can remain aloft for years at a time; the swift, for example, spends nearly its entire life in the air while landing only to breed. Along with many other animals (for example dolphins, whales), swifts evolved to be able to put one side of their brain to sleep at a time, so that they can sleep in the air while not actually being unconscious, see Lapierre et al. [2007]. What is common among these examples is not only the evolved capability of the high efficiency flight, but also the unique ability to manage energy that

is implemented by both the optimal energy expenditures and energy harvesting.

Considering the current state of the art in aerial robotics (algorithmic support, instrumentation, SWAP constraints), it is our firm belief that the best approach to enable long duration flight would combine the collaborative mission management and energy harvesting. Collaboration is the first key capability that spans across every element of the mission. First, collaboration enables effective search of available energy. Most of the available energy sources are not visible but detectable by intelligent robots equipped with appropriate sensors. Thus, multiple agents would have much better chances of finding "free energy" when cooperating and sharing their findings. Second, the operational utility of multiple agents equipped with complementary sensors is superior to the capability of an individual agent. Finally, robustness of the collaborative mission execution is significantly higher because partial loss of a subset of the vehicles does not lead to the loss of entire flock capability. Energy harvesting is the second complementary enabler of long endurance flight that enables accumulation of energy. The methods of energy extraction feasible for aerial application include the solar photovoltaic and airflow soaring that can be based on the convective air (thermaling) or wind shear energy extraction. While the photovoltaic boost can be achieved only during the daylight, the extraction of power of surrounded moving airflow can be utilized even during the nighttime. This combination is the ultimate solution for the "eternal" operational endurance.

Therefore, it is envisioned that enhancing mission performance while reducing its cost can be achieved by implementing energy harvesting and collaboration capabilities onboard of multiple autonomous solar-powered and thermal-soaring gliders. Thus, the triplet of (i) mission management, (ii) energy harvesting and (iii) collaboration builds the fundamental architecture of future energy enhanced autonomy. This architecture should be based on the distributed online execution of the following individual and distributed platforms' algorithms:

- Individual glider:
 - Integration of prior knowledge of the operational environment into effective collaborative search for energy;
 - Identification of the inherent flying qualities of each glider and detection of the environmental energy excess (convective thermal or wind shear) which are based on the total mechanical energy (the sum of kinetic and potential energy);
 - Identification of parameterized mathematical models of energy sources and estimation and "mapping" of their dynamic motion;
 - Autonomous guidance to enable energy harvesting while in the vicinity of an energy source;
 - Optimization of solar energy gain and electrical energy storage while in thermal soaring flight;
 - Sharing of the environment knowledge and the current state of cumulative energy (stored in onboard batteries plus the total mechanical energy) of each glider;
- Flock of gliders:
 - Distributed mission planning and cooperative control of the flock as functions of mission objectives and the reported cumulative energy of the flock; local feedback

to the mission planner allows for timely update and adjustment;

- Estimation of the free energy density distribution in the operational environment;
- Adjustment of the scale of the mission (number and strategy of multiple agents) defined by the rate of total energy expenditure.

Since the number of involved algorithms and technologies is significant, the remainder of the paper briefly outlines the core ideas implemented to date in both the high-fidelity simulation and the real onboard hardware environments. Therefore, Section 2 describes the "individual gliders" algorithms as outline above. The following section 3 outlines the development of the collaborative autonomy algorithms. Section 4 provides necessary details of the system integration including the environment for verification and validation of the developed algorithms in high-fidelity simulation and experimental flight testing. The paper ends with a brief outline of the future development steps.

2. INDIVIDUAL GLIDERS ALGORITHMS

The algorithms of individual platforms are primarily responsible for the sustainable flight of a partially uncertain glider and exploration and sharing of knowledge about the environment. The algorithms run online and enable identification of the inherent flight dynamics properties of the glider which are in turn used to detect the thermal updrafts. When flying in the updraft the guidance algorithm is engaged to enable the maximum harvesting efficiency of the updraft's energy, and on the other hand estimates the updraft geometry and motion that are used to georeference the updraft and share its utility properties across the network of collaborative gliders. Besides the collaborative mission objective and initial mission plan, the georeferenced map is the formalized knowledge used in the collaborative mission replanning phase. While in autonomous soaring mode, the electrical management system that consists of solar panels, batteries and the maximum energy tracking circuitry, supports the avionics and recharges the batteries keeping them evenly balanced. At any given time each individual platform can be either in a search or in a soaring mode. While the soaring mode is primarily defined by the energy gain objective, the search mode is driven by the intelligent algorithm that combines the goals of the distributed mission and the need to search for energy sources in the environment. Development of these intelligent algorithms that enable optimal balancing of energy gain and mission objectives is the most promising direction of the current and future research.

2.1 Glider Identification and Updraft Detection

There is a number of prior efforts devoted to the autonomous soaring capability. First demonstrated by human pilots in 1900s (see Simons and Schweizer [1998]) the idea of soaring in convective air became feasible for onboard autonomous implementation only in the 1990s, see Wharington [1998]. While enabling the desired functionality by primarily mimicking the birds flight and indeed achieving significant extended flight capabilities (see Edwards [2008], Allen [2006] and Allen and Lin [2007]), most of the algorithms implemented significant portion of

heuristic in the identification of the updraft strength, its potential utility in energy gain, and the decision of when and how to enter the updraft. The reason for employing heuristic approaches is obvious, since both the strength of the updraft and its efficiency are both subject to significant uncertainties. First, they result from the uncertain flight characteristics of the specific glider no matter how well the airframe is modeled and flight tested; significant advances in material and structures sciences produce novel airframes that are strong and flexible on one hand, and therefore aerodynamically uncertain when bend and twisted on the other hand. Second, when a glider is propelled through the unsteady air the updraft estimation algorithm lacks of spatial content (both in horizontal and vertical directions) in the noisy measurements of the vertical velocity of convective air. Thus, for any given altitude of flight it takes essential time before the updraft geometry is identified and the guidance algorithm is engaged. It is worth noting that when controlled by the thermal centering guidance law the estimation algorithm partially regains the spatial data in horizontal direction. To successfully identify the thermal strength in vertical direction it would take prohibitively long time for a single glider, thus to achieve rapid identification of 3D energy profile of any given thermal updraft it is very effective to utilize a number of collaborative platforms simultaneously sampling the same updraft in three dimensions.

While adapting the conceptual ideas of autonomous soaring, the approach used in our development shifts the focus from heuristics toward the online estimation algorithms of the glider flight dynamics and the parameterized model of the convective updraft. The algorithm of detecting a thermal is based on combining two complementary approaches; however conceptually they are similar as they compare the natural metrics of the system with the same actually measured characteristics of the glider. The first approach utilizes the inherent sink rate polar and the second one is based on the total energy of the system.

The sink rate polar is the curve of the vertical speed plotted versus the true air speed (TAS). Every glider has a very specific sink polar as it reflects the glider inherent ability to descend in wings level flight in no-wind conditions; sink polar can be obtained to characterize the sink rate at various bank angles that can be used to minimize the energy loss in turning flight. Thus, if the sink polar is known then the difference between the actually measured sink rate and the point on the sink polar corresponding to the measured true air speed identifies if there is an excess of energy in the air that forces the glider away from its native sink polar; the sign of the difference defines the updraft and downdraft conditions. Implementation of this approach depends on precise characterization of the sink polar of the glider that can be practically achieved in extensive experimentation. However, experimentation can hardly provide an ideal controlled conditions, and in every flight of the same platform there are always subtle differences that are not accounted for. Based on the extensive experimental data collected on a number of flights (see Andersson et al. [2012b] and the references herein) in close to ideal no-wind conditions the sink polar was first obtained off-line. Analysis of the measurements confirmed that the sink polar can be represented by a second order

polynomial $V_s = A \cdot V_{tas}^2 + B \cdot V_{tas} + C$ with coefficients A, B , and C defined by the least squares approximation method; similar results can be found in Reichmann and Bishop [1978], Edwards [2008]. The same method is then implemented onboard as a recursive least square (RLS) estimator, see Astrom and Wittenmark [1975], to account for any variations in the setup of the actual flying platform. An example of the experimental data and the resulting approximation is presented in Figure.1.

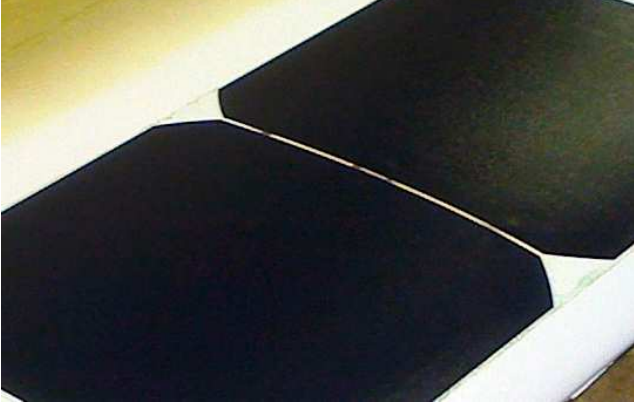


Fig. 1. Identifying the inherent sink polar: both the vertical and the TAS are directly measured by the onboard sensors. The online RLS result is slightly different but well within the decision making bounds.

The analytical representation of the sink polar contribute significantly not only to the identification of thermal updrafts but also to the mission planning of a particular glider, see Piggott [1997] and Administration [2011]. In particular, the polar defines the minimum sink rate $V_{s.min}$ and the corresponding speed command for the autopilot to follow. While $V_{s.min}$ is too close to the stall speed V_{stall} and should be avoided ($V_{stall} \approx V_{s.min}$), the effective speed commanded in thermaling mode V_{th} is slightly higher. The polar also defines the optimal TAS command V_{cc} for the maximum glide ratio that is used by the navigation task in planning for the maximum range "cross-country" segment. While the sink polar is obtained in no-wind environment, its application to the known wind conditions is straightforward and enables calculating distances to be traveled in cross-country flight, see more details in Piggott [1997] and Administration [2011].

The *total energy* approach is also widely used in human piloted soaring flight. It is based on the idea that at any given moment the mechanical energy E_{tot} of the soaring glider combines the potential $E_p = mgh$ and kinetic $E_k = \frac{m \cdot V^2}{2}$ energy of the airframe minus the "leakage" of the energy due to the work of the aerodynamic drag. For a relatively "clean" aerodynamic body the latter component can be neglected over a reasonably long period of time (tens of seconds). Therefore for the total energy and the rates of change one can consider the following:

$$\begin{aligned} E_{tot} &= mgh + \frac{m \cdot V^2}{2}, \quad E = \frac{E_{tot}}{mg}, \\ \dot{E} &= \frac{V \cdot \dot{V}}{g}, \quad \ddot{E} = \frac{\dot{V}^2 + V \cdot \ddot{V}}{g} + \ddot{h}, \end{aligned} \quad (1)$$

where m is the mass of the airframe, g is the gravitational constant, E is the normalized total mechanical energy of the system (also call specific energy), h is the height, and V is the inertial speed. Therefore, for highly efficient airframes the longitudinal long period oscillations represent the natural tradeoff of kinetic and potential energy while their sum remains constant. As a consequence, in no updraft conditions the rate of change of the total energy $\dot{E} \approx 0$. In turn, if there is a significant variation of the total energy, then the energy rate will be significantly away from zero thus indicating the energy increase $\dot{E} \gg 0$ due to an updraft or decrease $\dot{E} \ll 0$ due to the downward air flow; note that the inertial speed does not change so rapidly when meeting the convective vertical flows. All the components of equation (1) are readily available in onboard autopilot. Both equations in (1) are included into one Kalman filter along with the inertial and barometric sensors outputs. The resulting energy rate solution provides another precise indication of the updraft event. A comparison of the outputs of both approaches with the output of the total energy compensated variometer (TEK) \dot{h}_{TEK} is presented next in Figure.2.

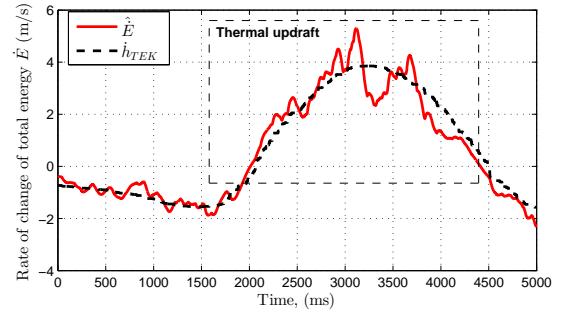


Fig. 2. Comparison of two approaches to the detection of thermal updrafts in mathematical model using Condor flight simulator, see Condor [2013]. Similar data is obtained in flight by utilizing the measurements of SkyAssistant TEK variometer from PitLab [2013]

The outcomes of the total energy estimator in (1) are used in the guidance law implementation that is presented next.

2.2 Guidance in Thermal Centering Mode

When a thermal updraft is detected the glider needs to perform an automatic maneuver to enable staying in the thermal with the objective of increasing the glider's potential energy through a rapid increase of the height. The theoretical development of the thermaling guidance law has been recently reported in Andersson et al. [2012b]). The most recent experimental results and findings that motivate further refinement of the solution were discusses in Andersson et al. [2012a]. This development was recently modified to include explicitly the sign of the turn rate command that is defined by the filtered value of the body measured roll rate p ; it was observed in a number of flights that entering the thermal induces the p rate that rolls the wings away from the thermal. The resulting thermaling guidance law implemented onboard of real glider enabled successful latching and effective exploitation of the thermal by rapidly raising flight altitude up to the ceiling of the updraft.

The thermal centering guidance law that produces a turn rate command $\dot{\psi}_c$ to the autopilot is based on the feedback control law that takes into account the desire to get closer to the updraft (defined by the ρ_d) where its intensity (vertical speed) is the highest, while balancing the turn rate and the turn-induced sink rate by a measure proportional to the rate of change of the total energy increase (defined by the \ddot{E} in (1)), see the geometry of the guidance task in Figure.3 and the resulting guidance law in (2):

$$\dot{\psi}_c = -\text{sign}(p) \cdot \left(\frac{V}{\rho_d} - k_1 \cdot \ddot{E} \right), \quad (2)$$

where ρ and ρ_d are the current distance and the desired orbital radius around the center of the thermal updraft, and k_1 is the feedback gain defined by the stability and performance requirements. For the feasibility of theoretical

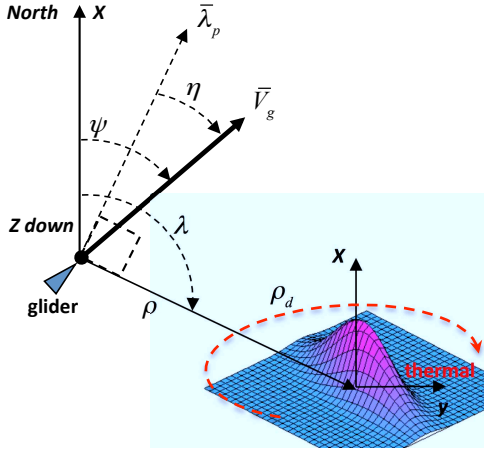


Fig. 3. Kinematics of guidance around a thermal updraft; the desired orbit is represented by the red dashed line defined by ρ_d .

development the thermal center is assumed stationary with its position unknown. The desired distance (ρ_d) toward the center at this point is not defined, however for the stability of the control law it is assumed to be away from zero. The best value of ρ_d is initially assigned based on statistical observations of the glider performance and the shapes of updrafts in the area. Later on when collaborative gliders contribute to the identification of the updraft geometry this value is updated, thus resulting in a feedback that improves the collaborative efficiency of utilizing the free energy of the updraft. For the stability analysis of the thermaling guidance law it is assumed that the intensity of the updraft can be represented by the Gaussian distribution function of the form:

$$\omega = \omega_p \cdot e^{-\left[\frac{(x-x_0)^2 + (y-y_0)^2}{2\sigma^2} \right]}, \quad (3)$$

where x_0, y_0 represent the unknown coordinates of the center of updraft, x, y represent the coordinates of the glider, ω_p is the peak intensity of the updraft, and σ define the geometry of the symmetric updraft (in general case $\sigma_x \neq \sigma_y$). For a stationary updraft modeled by Gaussian distribution function with $\sigma > 0$, $\omega_p > 0$ and the glider with $V > 0, \rho_d > 0$ it is proven that the feedback guidance law in (2) is locally asymptotically stable with an equilibrium at $(\eta, \rho - \rho_d) = (0, 0)$ and a region of

attraction $\Omega = \{(\eta, \rho - \rho_d) : |\rho - \rho_d| \leq \beta, |\eta| \leq \alpha\}$, where $\beta < \rho_d, \alpha < \pi/2$, for any

$$k_1 > \tan \alpha \frac{\sigma^2}{\omega_p(\rho_d - \beta)^2} e^{\left(\frac{-(\rho_d + \beta)^2}{2\sigma^2} \right)}$$

The physical meaning of the guidance law (2) is to increase the turn rate (typically implemented by the onboard autopilot through modifying the bank angle) till the rate of change of the increase of total energy is compensated by the sink resulted from the desire to get closer to the center of the thermal. In fact, the sink polar diagram (Figure.1) and the discussion come handy here as they show that the sink rate gradually increases with the bank angle of the glider.

It is realized however, that the thermals geometry and their motion is more complex: it is not only moving but also bending Reichmann and Bishop [1978]. Identification of the thermal motion is a separate task, to be performed effectively online the solution should integrate the knowledge gained by multiple gliders. As described above, the thermal intensity model adopted in this study is the 2-dimensional Gaussian distribution, and it can be argued whether this function is a good representation of a thermal or not. However, even if a Gaussian does not encompass all the features of an actual updraft, most sources seem to agree that it does capture many of the basic characteristics of a real thermal, i.e., being strongest at the core, with a rounded shape and gradual decrease in strength towards the edges; see, for example, Wharington [1998] and Pagen and Bryden [1992]. Still, the greatest uncertainty in the analysis can likely be contributed to the updraft model.

2.3 Identification of the Updraft Geometry

Identification of an updraft (strength and geometry) is performed online by each glider when the soaring guidance algorithm is engaged. The algorithm is based on probabilistic approach Bergman [1999].

3. COOPERATIVE ALGORITHMS

4. SYSTEM INTEGRATION ENVIRONMENT

5. FUTURE PLANS

Next we see a few subsections.

5.1 Review Stage

Please use this document as a template to prepare your manuscript. For submission guidelines, follow instructions on paper submission system as well as the Conference website.

Note that conferences impose strict page limits, so it will be better for you to prepare your initial submission in the camera ready layout so that you will have a good estimate for the paper length. Additionally, the effort required for final submission will be minimal.

Some words might be appropriate describing equation (4), if we had but time and space enough.

$$\frac{\partial F}{\partial t} = D \frac{\partial^2 F}{\partial x^2}. \quad (4)$$

A subsubsection This equation goes far beyond the celebrated theorem ascribed to the great Pythagoras by his followers.

Theorem 1. The square of the length of the hypotenuse of a right triangle equals the sum of the squares of the lengths of the other two sides.

Proof. The square of the length of the hypotenuse of a right triangle equals the sum of the squares of the lengths of the other two sides.

5.2 Final Stage

Authors are expected to mind the margins diligently. Conference papers need to be stamped with conference data and paginated for inclusion in the proceedings. If your manuscript bleeds into margins, you will be required to resubmit and delay the proceedings preparation in the process.

5.3 Page margins

All dimensions are in *centimeters*.

Margin settings			
Page	Top	Bottom	Left/Right
First	3.5	2.5	1.5
Rest	2.5	2.5	1.5

It is very important to maintain these margins. They are necessary to put conference information and page number for the proceedings.

5.4 Figures and PDF Creation

All figures must be embedded in the document. When you include the image, make sure to insert the actual image rather than a link to your local computer.. As far as possible, use standard PDF conversion tools Adobe Acrobat or Ghostscript give best results. **It is important that all fonts be embedded/subsetted in the resulting PDF.**

5.5 Copyright Form

IFAC will put in place an electronic copyright transfer system in due course. Please do not send copyright forms by mail or FAX. More information on this will be made available on IFAC website.

6. MATH

If you are using Word, use either the Microsoft Equation Editor or the MathType add-on for equations in your paper (Insert — Object — Create New — Microsoft Equation or MathType Equation). Float over text should not be selected. Of course LaTeX manages equations through built-in macros.

7. UNITS

Use either SI as primary units. Other units may be used as secondary units (in parentheses). This applies to papers in data storage. For example, write $15\text{Gb}/\text{cm}^2$ ($100\text{Gb}/\text{in}^2$).

An exception is when English units are used as identifiers in trade, such as 3.5 in disk drive. Avoid combining SI and CGS units, such as current in amperes and magnetic field in oersteds. This often leads to confusion because equations do not balance dimensionally. If you must use mixed units, clearly state the units for each quantity in an equation. The SI unit for magnetic field strength H is A/m. However, if you wish to use units of T , either refer to magnetic flux density B or magnetic field strength symbolized as $\mu_0 H$. Use the center dot to separate compound units, e.g., $A \cdot m^2$.

8. HELPFUL HINTS

8.1 Figures and Tables

Figure axis labels are often a source of confusion. Use words rather than symbols. As an example, write the quantity Magnetization, or Magnetization M , not just M . Put units in parentheses. Do not label axes only with units. As in Fig. 1, for example, write Magnetization (A/m) or Magnetization ($A \cdot m^{-1}$), not just A/m. Do not label axes with a ratio of quantities and units. For example, write Temperature (K), not Temperature/K.

Multipliers can be especially confusing. Write Magnetization (kA/m) or Magnetization (103 A/m). Do not write Magnetization (A/m) ? 1000 because the reader would not know whether the top axis label in Fig. 1 meant 16000 A/m or 0.016 A/m. Figure labels should be legible, approximately 8 to 12 point type.

8.2 References

Use Harvard style references (see at the end of this document). If you are using LaTeX, you can process an external bibliography database or insert it directly into the reference section. Footnotes should be avoided as far as possible. Please note that the references at the end of this document are in the preferred referencing style. Papers that have not been published should be cited as unpublished. Capitalize only the first word in a paper title, except for proper nouns and element symbols.

8.3 Abbreviations and Acronyms

Define abbreviations and acronyms the first time they are used in the text, even after they have already been defined in the abstract. Abbreviations such as IFAC, SI, ac, and dc do not have to be defined. Abbreviations that incorporate periods should not have spaces: write C.N.R.S., not C. N. R. S. Do not use abbreviations in the title unless they are unavoidable (for example, IFAC in the title of this article).

8.4 Equations

Number equations consecutively with equation numbers in parentheses flush with the right margin, as in (1). First use the equation editor to create the equation. Then select the Equation markup style. Press the tab key and write the equation number in parentheses. To make your equations more compact, you may use the solidus (/), the exp function, or appropriate exponents. Use parentheses to

avoid ambiguities in denominators. Punctuate equations when they are part of a sentence, as in

$$\int_0^{r_2} F(r, \varphi) dr d\varphi = [\sigma r_2 / (2\mu_0)] \cdot \int_0^{\inf} \exp(-\lambda |z_j - z_i|) \lambda^{-1} J_1(\lambda r_2) J_0(\lambda r_i) d\lambda \quad (5)$$

Be sure that the symbols in your equation have been defined before the equation appears or immediately following. Italicize symbols (T might refer to temperature, but T is the unit tesla). Refer to (1), not Eq. (1) or equation (1), except at the beginning of a sentence: Equation (1) is

8.5 Other Recommendations

Use one space after periods and colons. Hyphenate complex modifiers: zero-field-cooled magnetization. Avoid dangling participles, such as, Using (1), the potential was calculated. [It is not clear who or what used (1).] Write instead, The potential was calculated by using (1), or Using (1), we calculated the potential.

A parenthetical statement at the end of a sentence is punctuated outside of the closing parenthesis (like this). (A parenthetical sentence is punctuated within the parentheses.) Avoid contractions; for example, write do not instead of dont. The serial comma is preferred: A, B, and C instead of A, B and C.

9. CONCLUSION

A conclusion section is not required. Although a conclusion may review the main points of the paper, do not replicate the abstract as the conclusion. A conclusion might elaborate on the importance of the work or suggest applications and extensions.

ACKNOWLEDGEMENTS

Partially supported by the Roman Senate.

REFERENCES

Federal Aviation Administration. *Glider Flying Handbook*. JL Aviation LLC, 2011.

Michael J Allen. Updraft model for development of autonomous soaring uninhabited air vehicles. In *Forty Fourth AIAA Aerospace Sciences Meeting and Exhibit*, 2006.

Michael J Allen and Victor Lin. Guidance and control of an autonomous soaring vehicle with flight test results. In *AIAA Aerospace Sciences Meeting and Exhibit, AIAA Paper*, volume 867, 2007.

Klas Andersson, Kevin Jones, Vladimir Dobrokhodov, and Isaac Kaminer. Thermal highs and pitfall lows-notes on the journey to the first cooperative autonomous soaring flight. In *Decision and Control (CDC), 2012 IEEE 51st Annual Conference on*, pages 3392–3397. IEEE, 2012a.

Klas Andersson, Isaac Kaminer, Vladimir Dobrokhodov, and Venanzio Cichella. Thermal centering control for autonomous soaring; stability analysis and flight test results. *AIAA Journal of Guidance, Control, and Dynamics*, 35(3):963–975, 2012b.

KJ Astrom and Björn Wittenmark. *Adaptive control*. Addison-Wesley, 1975.

Niclas Bergman. *Recursive Bayesian Estimation*. PhD thesis, Department of Electrical Engineering, Linköping University, Sweden, 1999.

Condor. The competition soaring simulator, 2013. URL <http://www.condorsoaring.com/>.

Daniel J Edwards. Implementation details and flight test results of an autonomous soaring controller. In *AIAA Guidance, Navigation and Control Conference and Exhibit*. North Carolina State University, 2008. AIAA 2008-7244.

Jennifer L Lapierre, Peter O Kosenko, Oleg I Lyamin, Tohru Kodama, Lev M Mukhametov, and Jerome M Siegel. Cortical acetylcholine release is lateralized during asymmetrical slow-wave sleep in northern fur seals. *The Journal of Neuroscience*, 27(44):11999–12006, 2007.

David R Martinez, Robert A Bond, and M Michael Vai. *High performance embedded computing handbook: A systems perspective*. CRC Press, 2008.

Kenzo Nonami, Muljowidodo Kartidjo, Kwang-Joon Yoon, and Agus Budiyo. *Autonomous Control Systems and Vehicles: Intelligent Unmanned Systems*. Springer Publishing Company, Incorporated, 2013.

Dennis Pagen and B Bryden. *Understanding the sky*. Black Mountain Books, 1992.

Derek Piggott. *Gliding: A handbook on soaring flight*. A & C Black, 1997.

PitLab. The competition soaring simulator, 2013. URL <http://www.pitlab.com>.

Helmut Reichmann and Max Bishop. *Cross-country soaring, Soaring Society of America*. Thomson Publications, 1978.

Philip L Richardson. How do albatrosses fly around the world without flapping their wings? *Progress in Oceanography*, 88(1):46–58, 2011.

Bruno Siciliano and Oussama Khatib. *Springer handbook of robotics*. Springer, 2008.

Martin Simons and Paul A Schweizer. *Sailplanes by Schweizer: A History*. Crowood Press, 1998.

Gaurav Singh and Sandeep Kumar Shukla. *Low Power Hardware Synthesis from Concurrent Action-Oriented Specifications*. Springer, 2010.

Ho-Ming Tong. Microelectronics packaging: present and future. *Materials chemistry and physics*, 40(3):147–161, 1995.

USGS. Bird completes epic flight across the pacific. ScienceDaily, September 2007.

John Wharington. *Autonomous control of soaring aircraft by reinforcement learning*. PhD thesis, Royal Melbourne Institute of Technology (Australia), 1998.